Computational study on the mechanism of metal-free photochemical borylation of aryl halides

Chenhao Tu, Nana Ma, Qingli Xu, Wenyue Guo, Lanxin Zhou, and Guisheng Zhang

Correspondence to: Nana Ma (E-mail: *mann076@htu.edu.cn*); Guisheng Zhang (E-mail: *zgs@htu.edu.cn*)

School of Chemistry and Chemical Engineering, Henan Key laboratory of Organic Functional Molecule and Drug Innovation, Henan Key Laboratory of Boron Chemistry and Advanced Energy Materials, Key Laboratory of Green Chemical Media and Reactions, Ministry of Education, Henan Normal University, Xinxiang, Henan, 453007, China

ABSTRACT

C-radical borylation is an significant approach for the construction of carbon−boron bond. Photochemical borylation of aryl halides successfully applied this strategy. However, precise mechanisms, such as the generation of aryl radicals and the role of base additive(TMDAM) and water, remain controversy in these reactions. In this study, photochemical borylation of aryl halides has been researched by density functional theory (DFT) calculations. Indeed, the homolytic cleavage of the C–X bond under irradiation with UV-light is a key step for generation of aryl radicals. Nevertheless, the generation of aryl radicals may also undergo the process of single electron transfer and the heterolytic carbon-halogen bond cleavage sequence, and the latter is favorable during the reaction.

1. Introduction

Aryl boronic acid and its derivatives have been widely used in synthesis applications of chemical[1-2], pharmaceutical[3-4] and material[5-6]. Therefore, methods that can efficiently, economically and environmentally synthesize aryl borate, especially functional aryl borate, is urgently needed by researchers.

In the past, the synthesis of alkyl or aryl boronic esters can be obtained by reaction between metal organic reagents (Li, Mg) and boron reagents.[7-13] but these reactions are far from being ideal. Then, the borylation with transition metals (Ni, Cu, Zn, Pd) as a catalyst has been an effective methods to convert C-X bonds into C-B bonds.[14-15] Recently, a direct C–H bond borylation method based on transition metal catalysts (Ru, Rh, Ir) has also been developed.[16-19] In addition, a complementary method has also been developed, which is achieved through C-radical borylation.[20] These type of reactions uses diboron reagents such as $B_2(pin)_2$, $B_2(cat)_2$ and $B_2(neop)_2$ as boron reagents. All these compounds can interact with Lewis bases or free radical intermediates due to owning two empty p(B) orbitals which is the basis for the successful C-radical borylation. The methods can obtain the corresponding boronic acid derivatives from various readily available chemical raw materials under relatively mild reaction conditions. However, all these methods suffer some drawbacks such as limited functional group tolerance, higher costs, or the necessity of rigorous anhydrous conditions. On the other hand, with the increasing awareness of sustainable development in synthetic chemistry, photochemical borylation was turned to be an ideal enabling technology.[21] In 2016, Li and coworkers reported a novel and efficient photolytic borylation reaction of aryl iodide and bromide by using light as a clean reagent.[22-24] This photochemical borylation of aryl halides and bromide using $B_2(pin)_2$ and a Lewis-basic activator TMDAM (N,N,N',N'-tetramethyl-

diaminomethane) in aqueous solution at low temperatures (Figure 1).

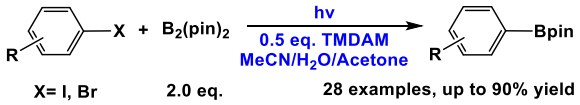

Figure 1. Summary of borylation reaction of aryl iodide/bromide induced by UV- light.

From the reaction results, this metal-free reaction features very mild conditions, short reaction times, generally high yields and broad functional group tolerance. It is complementary to the existing C-B bond formation methods. There are several important experimental details of this work. (i) Initially, a solution of 4-iodoanisole and diboron in acetonitrile was irradiated with a 300 W high pressure mercury lamp (maximum at 365 nm) for 4 hours. The desired aryl-B(pin) product was formed in 29% yield. In the absence of light, no conversion was observed. It is no doubt that UV-light plays an important role in this reaction; (ii) Adding water and acetone as co-solvents was beneficial and increased the yield to 46% which suggests that water may be involved in reaction; (iii) Experiments shows that an organic base, TMDAM, could futher improve the yield to 58%. (iv) Using two equivalents of $B_2(pin)_2$ improved the yield to 72%; (v) A series of controlled experiments shows that when TEMPO was added as a radical scavenger, the conversion was low. Furthermore, a hydrogen atom donor, Bu_3SnH, increased the conversion but led to anisole as the major product. It indicates that this reaction proceeds in the form of free radical reaction, and aryl radical is an important intermediate.

However, the mechanism of photochemical borylation of aryl halides remains elusive. In order to gain insight into the reaction mechanism, and particularly to probe the role of water, additives (TMDAM) and light, computational efforts are made to study the mechanism of this photochemical borylation reaction by using density functional theory (DFT) methods.

2. Computational Methods

The quantum chemical calculations were carried out employing Gaussian 09 program package[25]. The structures, including the reactants, intermediates, transition states (TS), and corresponding products in the research system were calculated using the B3LYP[26] functional with the 6-31G(d) (for C, H, O, N, B) basis set and SDD[27] (for I) basis set to perform full geometry optimization. Calculations throughout this paper were performed on the full structures of the reported compounds, rather than their truncated models. For all the optimized geometries, the frequency analysis calculations were carried out at the same level to characterize the stationary points to be minima (no imaginary frequency) or transition states (only one imaginary frequency). An intrinsic reaction coordinate (IRC)[28] calculation was performed to identify transition state uniquely connecting the reactant to product. In addition, the solvent effects were considered in the acetonitrile solvent by using the SMD model[29-31] to mimic the experiment condition. On the basis of the optimized structures, the solvent-corrected free energies were obtained adopting the B3LYP functional with the D3 version of Grimme's dispersion[32-35], coupled with the 6-311++G(d, p) (for C, H, O, N, B) basis set and SDD (for I) basis set. The Gibbs free energy changes (ΔG^0) and corrected Gibbs activation energies ($\Delta G^{0\ddagger}$) (kcal/mol at 298 K) were used to discuss the photochemical borylation reaction.

3. Results and Discussion

The controlled experiments showed that the aryl radical is an important intermediate in the reaction process. A preliminary mechanism was proposed by Li et al to disclose some mechanistic information in this radical borylation process triggered by ultraviolet light (Figure 2).

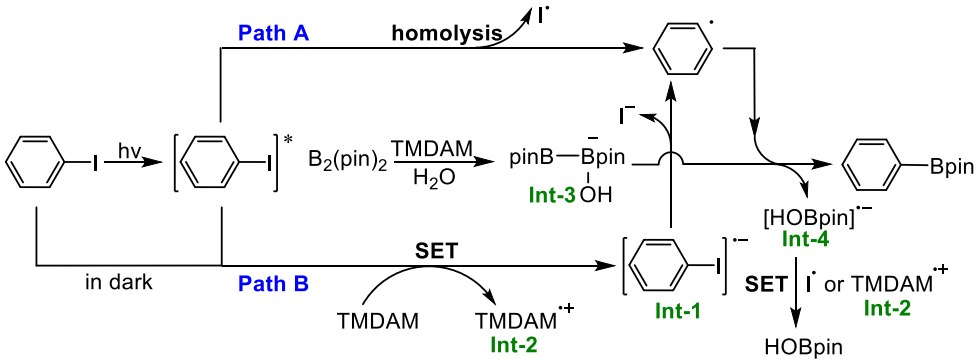

Figure 2. Reaction mechanism proposed by Li et al.

They proposed two possible pathways for the formation of aryl radical by taking iodobenzene as an example. In path A, iodobenzene is excited from ground state to excited state when exposed to UV light, and then, aryl radical and iodine atom can be obtained through homolytic cleavage of C–I bond. In path B, single electron transfer (SET) process can occur between iodobenzene and TMDAM, and give radical anion Int-1 and radical cation Int-2. The resulting Int-1 generates aryl radical and iodine atom through heterolytic cleavage of C–I bond. Moreover, they thought TMDAM can activate a water molecule and further interact with $B_2(pin)_2$ to form the sp^3-sp^2 diboron species Int-3 under aqueous conditions. Int-3 can react with aryl radical to generate the target product PhBpin and radical anion Int-4. Then iodine atom or Int-2 can react with the resulting Int-4 through SET process to afford HOBpin as a byproduct. In order to investigate the mechanism of this interesting transformation, we verified path A and B by theoretical calculation at first. The results are shown below.

3.1 Possible reaction pathways of the generation of aryl radical at the stage of photoinitiation.

As a radical reaction induced by UV-light, the possible reactions in the photoinitiation stage should be determined first. Therefore, we use DFT methods to explore the feasibility of paths A and B proposed by Li et al.

For path A, the computed results showed that the excitation energy of iodobenzene from the ground state to the triplet excited state by absorbing energy provided from UV-light (55.8 kcal/mol, Figure 3a). After then, homolytic cleavage of C–I bond in excited State [Ph-I]* to generate aryl radical and iodine atom have a ΔG^0 value of 0.1 kcal/mol. This shows that this

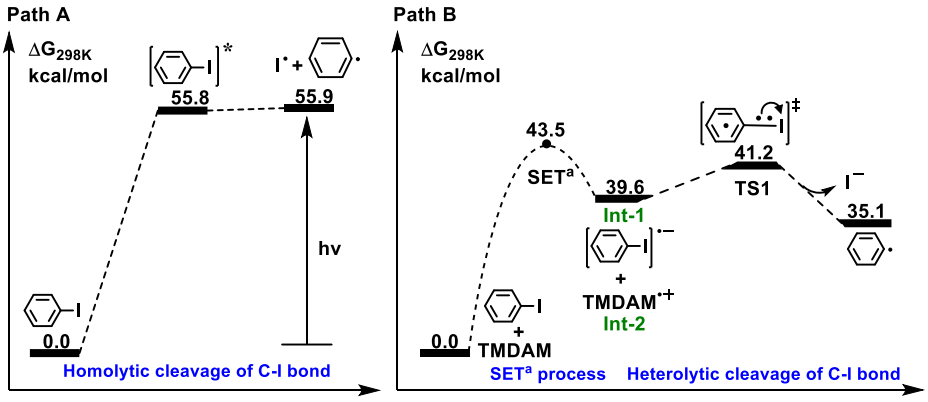

Figure 3. Possible reaction pathways of Ph-I at the stage of photoinitiation.

process can proceed under UV-light. In addition, Heterolytic cleavage of C–I bond was also considered and the ΔG^0 value is 2.4 kcal/mol for singlet (23.3 kcal/mol for triplet) (Figure S1) which is higher than homolytic cleavage.

For path B, Based on the Marcus electron transfer theory[36-37], the calculated activation barrier of SET[a] step between iodobenzene and TMDAM is 43.5 kcal/mol, PhI facilitate the oxidation of TMDAM to deliver $TMDAM^{\cdot+}$(Int-2). Specifically, the SET step have a ΔG^0 value of 39.6 kcal/mol results in radical anion Int-1 and radical cation Int-2, which illustrates that this process hardly occurs at room temperature. Comparatively, it can be concluded that aryl radical is more likely to be generated via homolysis of C–I resulting from photoexcitation. However, it is worth noting that heterolytic cleavage of C–I bond in Int-1 is easy to occur. This process can generate aryl radical and iodine atom with a $\Delta G^{0‡}$ value of 1.6 kcal/mol and a ΔG^0 value of -4.5 kcal/mol. So there is a possibility that the suitable electron donor will allow path B to occur.

In next section, the aryl radical borylation to produce the arylboron compound was explored by starting from borane reagent $B_2(pin)_2$.

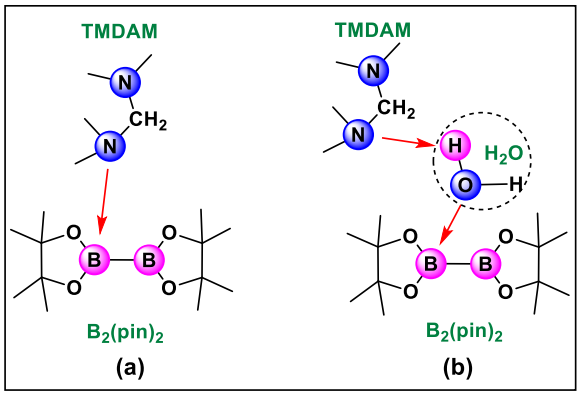

Figure 4. Coordination modes of $B_2(pin)_2$ with TMDAM/TMDAM+H_2O.

It is well established that Lewis bases can coordinate with $B_2(pin)_2$ in which boron atom has vacant p orbital to provide corresponding sp^3-sp^2 diboron adducts. Here, organic base TMDAM can interact with $B_2(pin)_2$ directly due to Lewis basicity of nitrogen atom (Figure 4a). Alternatively, experiments showed that water is beneficial for borylation with higher yield, and thus H_2O could be a bridge to connect diboron $B_2(pin)_2$ and TMDAM (Figure 4b), based on the Lewis properties of $B_2(pin)_2$, TMDAM and H_2O.

3.2 Interaction of TMDAM/TMDAM+H_2O with $B_2(pin)_2$ followed by introduction of aryl radical.

As shown in Figure 5, direct mode (a) that TMDAM interact with $B_2(pin)_2$ was taken into consideration. This interaction process has a $\Delta G^{0‡}$ value of 15.5 kcal/mol by transition state TS2, which gives complex Int-5 with a ΔG^0 value of 13.1 kcal/mol. For the indirect mode (b), the formation of complex Int-6 has a $\Delta G^{0‡}$ value of 17.1 kcal/mol and a ΔG^0 value of 15.6 kcal/mol, which is higher than that of complex Int-5 in absence of water. Due to the donor-acceptor interaction between $N^{\delta-}$ in TMDAM and $B^{\delta+}$ in $B_2(pin)_2$, one H–O bond in water molecule is polarized and further heterolysis affording cation Int-7 and anion Int-3 as proposed by Li et al., and this heterolysis process is slightly endothermic by 2.9 kcal/mol. To afford the borylation compound PhBpin, the following reaction of complex Int-5 or Int-6 with the resulting aryl radical under UV-light irradiation was investigated.

Starting from Int-5, the aryl radical attacks the sp^2-B of Int-5 to afford PhBpin along with a radical intermediate Int-8. This step has a $\Delta G^{0‡}$ value of 10.7 kcal/mol and a ΔG^0 value of -25.5 kcal/mol. For complex Int-6, as mentioned above, an easy heterolysis can afford anion Int-3 along with cation Int-7. Therefore, two possible reactions with aryl radical were considered. One is that aryl radical attacks the sp^2-B in Int-6 by climbing a $\Delta G^{0‡}$ value of 10.4 kcal/mol, leading to radical anion Int-9 along with intermediate Int-7 and HOBpin. The ΔG^0 value of this process is -61.3 kcal/mol. Alternatively, heterolysis product Int-3 reacts with aryl radical to afford Int-9 along with HOBpin, and this step has a $\Delta G^{0‡}$ value of 10.2 kcal/mol and a ΔG^0 value of -64.4 kcal/mol.

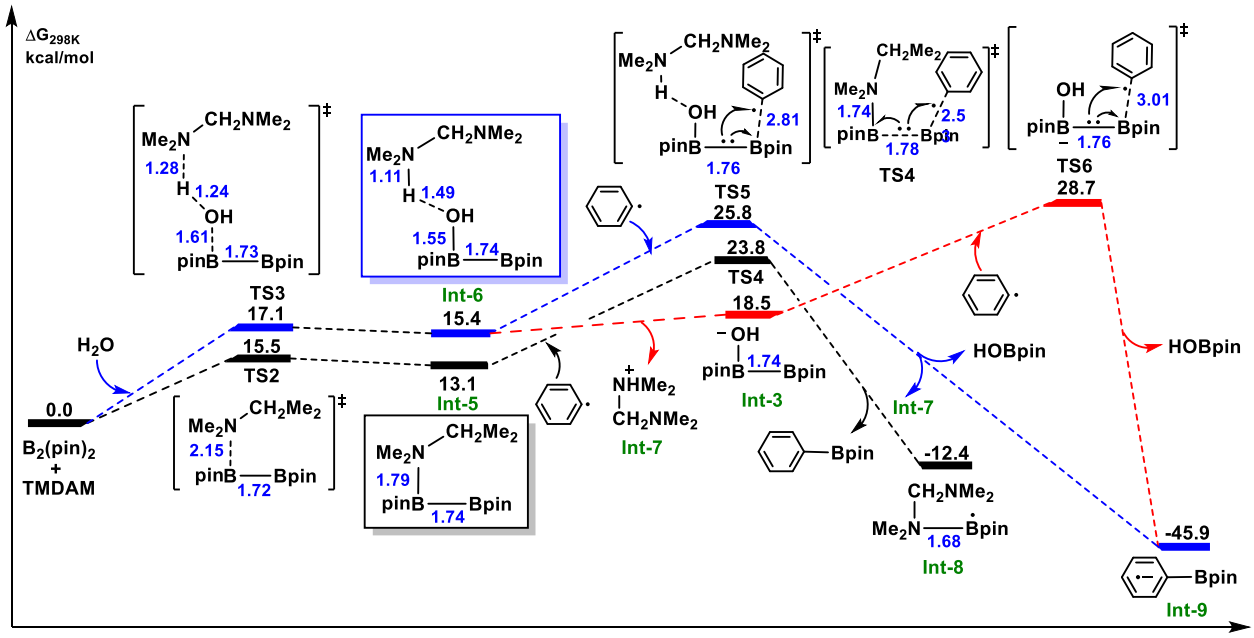

Figure 5. Possible reaction pathways of $B_2(pin)_2$ at the photoinitiation stage (bond distance Å in blue).

The radical anion Int-9 can be further oxidized by resulting iodine atom or substrate iodobenzene via a SET process to form target product PhBpin (SET[b], SET[c], Figure S2 in SI), and the activition energy barrie is 16.1 kcal/mol and 1.9 kcal/mol, respectively.

Comparatively, for the possible reaction of diboron adducts with potential aryl radical to generate PhBpin, the pathway starting from Int-5 seems to be more favorable, because the $\Delta G^{0\ddagger}$ value is 23.8 kcal/mol which is lower than those of pathways starting from Int-6 and Int-3 (25.8 kcal/mol and 28.7 kcal/mol). However, the role of water on the higher yield cannot be explained. Therefore, more reliable pathways need to be investigated.

Aryl radical and iodine atom can trigger a chain transfer and cause more molecules to participate in the reaction.[38-43] Therefore, beyond the formation of diboron adduct followed by reaction with aryl radical, we considered that $B_2(pin)_2$ may trap aryl radical or Iodine atom generating boryl radical and then reacts with TMDAM/TMDAM + H_2O.

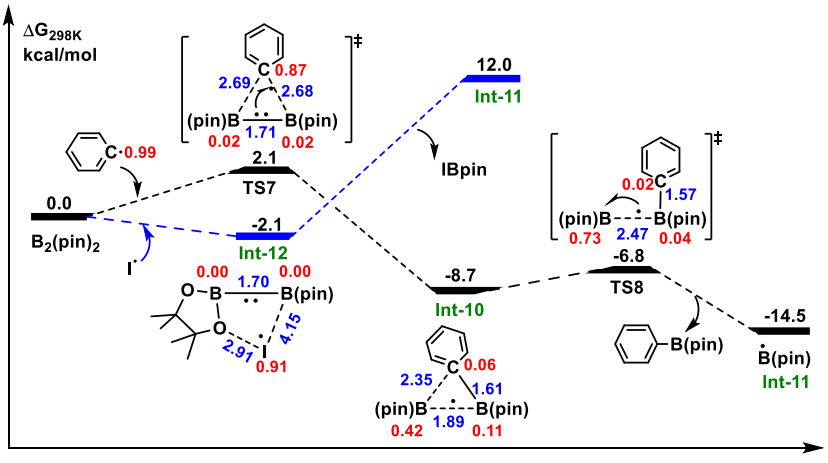

Figure 6. Trapping of aryl radical with $B_2(pin)_2$ (bond distance Å in blue, spin density in red).

3.3 Trapping of aryl radical with $B_2(pin)_2$.

As shown in Figure 6, aryl radical can simultaneously attack two sp^2-B atoms in $B_2(pin)_2$ by a three-membered transition state TS7 in which the distance of C–B is 2.7 Å and bond length of B–B (1.71 Å) change hardly, leading to an intermediate Int-10 in which formation of C–B bond (1.61 Å) and elongation of B–B bond (to 1.89 Å).

Subsequently, cleavage of weak B–B bond occurs in Int-10 leading to borylation product PhBpin along with boryl radical Int-11. This process has a lower $\Delta G^{0‡}$ value of 2.1 kcal/mol and a ΔG^0 value of -14.5 kcal/mol. Moreover, a detailed spin density distribution for the transition states (TS7 and TS8) and intermediate Int-10 further described the electronic process of C–B formation and B–B cleavage. As shown in Figure 6, the spin density of C decrease by 0.87 (in TS7)→0.06 (in Int-10) → 0.02 (in TS8), and simultaneously spin density of B-B undergoes 0.02-0.02 (in TS7) → 0.42-0.11 (in Int-10) → 0.73-0.04 (in TS8).

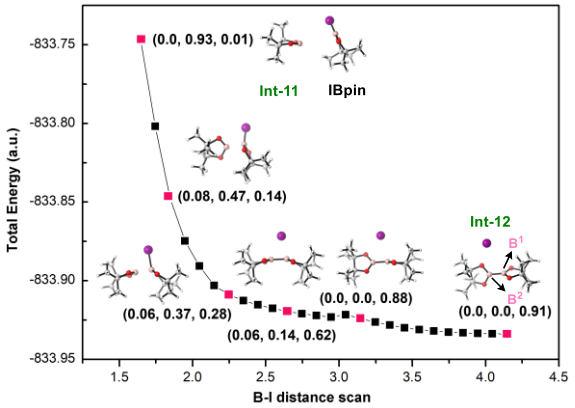

Figure 7. Variation tendency of energy and spin density (B1, B2, I) along the distance (in Å) of B1—I bond.

On the other hand, iodine atom reacts with $B_2(pin)_2$ to form complex Int-12 with exothermic by 2.1 kcal/mol. Int-12 can be converted to IBpin and Boryl radical Int-11 (Figure 6). For the process of Int-12 → Int-11 + IBpin, the transition state is in absence according to geometric and electronic structures optimized by flexible scan skill. As displayed in Figure 7, the changes on geometry and spin density of B1, B2, and I atoms illustrates that Int-12 decomposes into Int-11 and IBpin endothermically by 14.1 kcal/mol.

Boryl radical Int-11 is the key intermediate for the next catalytic cycle. However, Int-11 can be eliminated by coupling with iodine atom leading to IBpin, which can inhibit the chain transfer and terminate the reaction. The reaction between iodine atom and the boryl radical can give IBpin exothermically by 76.9 kcal/mol (Figure 8). Therefore, for a sustained borylation, continuous UV-light is necessary to active substrate iodobenzene to generate borylation product PhBpin along with boryl radical Int-11. However, experiment showed using two equivalents of $B_2(pin)_2$ could improve the yield of borylation product. It suggests that Iodine atom can be trapped by excess $B_2(pin)_2$ at the photoinitiation. By contrast, the resulting Iodine atom should be consumed by $B_2(pin)_2$ at the initial step rather than be trapped by boryl radical Int-11, the former is benefit for the free radical reactions.

3.4 Boryl radical Int-11 interact with TMDAM /TMDAM + H_2O.

Int-11 can interact with TMDAM /TMDAM + H_2O to generate an electron donor (with an single electron). The single electron can be transferred to the substrate iodobenzene generating radical anion Int-1. Int-1 can be converted to aryl radical easily (Figure 3, TS1, 1.6 kcal/mol).

Int-11 interact with TMDAM.

For this step, Int-11 interacts with TMDAM to afford complex Int-8 with ΔG^0 value of -12.4 kcal/mol. The required $\Delta G^{0‡}$ value for this step is 8.2 kcal/mol (Figure 8). Then, Int-8 can facilitate the reduction of iodobenzene to deliver $[Ph\text{-}I]^{-\cdot}$ (Int-1) and oxidized species Int-14 with ΔG^0 value of -40.6 kcal/mol. Based on Marcus electron transfer theory, the activation energy barrier of this SET step (SET^1) was calculated to be 25.3

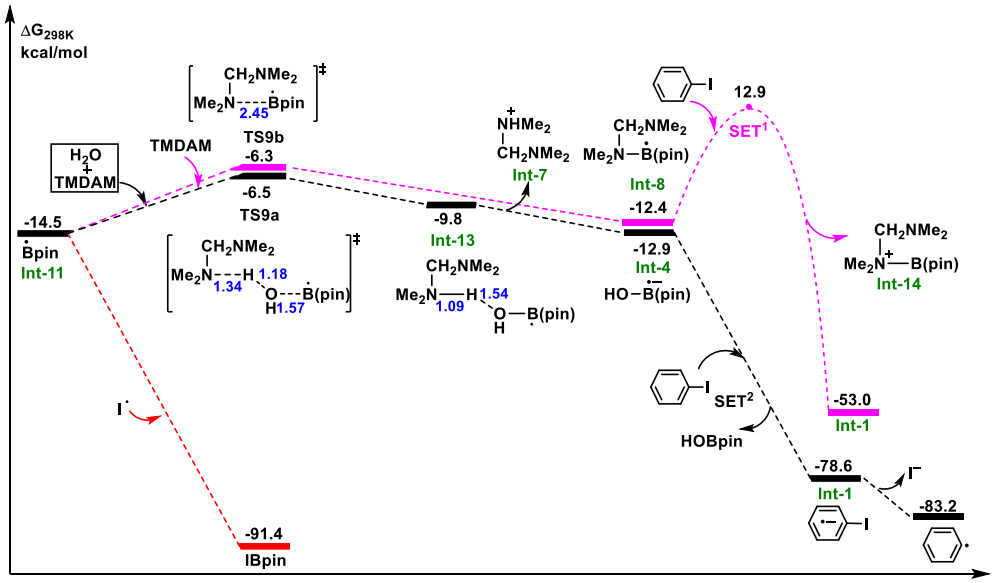

Figure 8. Generation of aryl radicals through SET process (bond distance Å in blue).

kcal/mol. Considering the slightly higher energy barrier and the promoting effect of water on this reaction, we thus investigated the pathway involved with water molecule.

Int-11 interact with TMDAM and H_2O.

When H_2O participates in this procedure, an intermediate Int-13 in which H-O distance is 1.54 Å can be afforded with a $\Delta G^{0‡}$ value of 8.0 kcal/mol. Int-13 further decompose into Int-4 and Int-7 with a ΔG^0 value of -12.9 kcal/mol. The following SET^2 process between Int-4 and PhI leading to Int-1 and HOBpin. This process is feasible with a ΔG^0 value of -65.7 kcal/mol, and we believe this SET^2 step is no barrier.

To specify this no barrier SET^2 process, we evaluated the energy profile by optimizing the complex Int-3···PhI as shown in Figure 9. The energy curve accompanied by C-I distance (from 2.16 to 3.16) and spin density of I, C and B (from 0.51, 0.19, 0.24 to 0.0, 0.83, 0.07) suggest that this SET^2 step is a process of decreasing energy. This shows that the presence of water is beneficial to SET process. So the presence of water is favorable for the reaction, which is consistent with the experimental result.

Subsequently, heterolytic cleavage of C-I bond in Int-1 generates Aryl radical along with I^- exothermically by 4.6 kcal/mol. Therefore, a cyclic chain transfer is formed and the free energy barrier for determining step is only 8.0 kcal/mol.

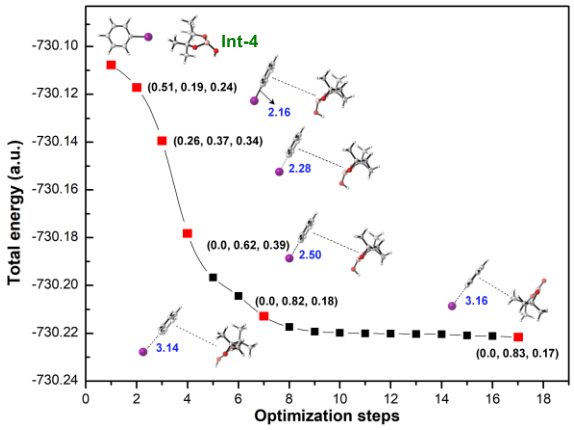

Figure 9. Variation tendency of energy and spin density (B, C, I) in SET^2 process.

4. Conclusions

Our computational studies suggest that the photochemical borylation of aryl halides could proceed as a cyclic radical chain transfer and the mechanism involves single electron transfer process. That is, initially aryl radical can be generated along with iodine atom by UV irradiation of iodobenzene. The following circular process consists of four steps. (i) $B_2(pin)_2$

traps aryl radical to afford the target product along with boryl radical Int-11, and another one $B_2(pin)_2$ traps Iodine radical. (ii) Interaction among Int-11, TMDAM and H_2O gives an electron donor intermediate Int-4. (iii) The single electron transfer process occurs between Int-4 and PhI to generate radical anion Int-1 along with by-product HOBpin. (iv) Heterolytic cleavage of C-I bond in Int-1 leads to aryl radical which can activate substrate $B_2(pin)_2$ directly. In this circular case, it is favorable to generate aryl radical through the cycle.

Acknowledgments

This work is financially supported by the National Natural Science Foundation of China (grant no. 21603062) and the 111 Project (D17007). The calculations are supported by the High Performance Computing (HPC) Centre of Henan Normal University.

Keywords: Aryl halides •C-radical borylation • Photochemical • Single electron transfer • DFT

Additional Supporting Information may be found in the online version of this article.

References and Notes

1. H. S. Ban, H. Nakamura, *Chem. Rec.*, **2015**, *15*, 616.
2. D. B. Diaz, A. K. Yudin, *Nat. Chem.*, **2017**, *9*, 731.
3. N. Huang, X. Ding, J. Kim, H. Ihee, D. A. Jiang, *Angew.Chem., Int. Ed.*, **2015**, *54*, 87040.
4. Y. Shoji, Y. Ikabata, Q. Wang, D. Nemoto, A. Sakamoto, N. Tanaka, J. Seino, H. Nakai, T. Fukushima, *J. Am. Chem.Soc.*, **2017**, *139*, 2728.
5. D. G. Hall, WILEYVCH, Weinheim, 2nd edn, **2011**.
6. C. Sandford, V. K. Aggarwal, *Chem. Commun.*, **2017**, *53*, 5481.
7. Y. Nagashima, R. Takita, K. Yoshida, K. Hirano, M. Uchiyama, *J. Am. Chem. Soc.*, **2013**, *135*, 18730.
8. S. K. Bose, K. Fucke, L. Liu, P. G. Steel, T. B. Marder, *Angew. Chem., Int. Ed.*, **2014**, *53*, 1799.
9. A. J. Warner, J. R. Lawson, V. Fasano, M. J. Ingleson, *Angew. Chem., Int. Ed.*, **2015**, *54*, 11245.
10. C. Zarate, R. Manzano, R. Martin, *J. Am. Chem. Soc.*, **2015**, *137*, 6754.
11. T. C. Atack, S. P. Cook, *J. Am. Chem. Soc.*, **2016**, *138*, 6139.
12. L. Zhang, L. Jiao, *J. Am. Chem. Soc.*, **2017**, *139*, 607.
13. T. Yoshida, L. Ilies, E. Nakamura, *ACS Catal.*, **2017**, *7*, 3199.
14. F. Mo, Y. Jiang, D. Qiu, Y. Zhang, J. Wang, *Angew. Chem., Int. Ed.*, **2010**, *49*, 1846.
15. S. Pietsch, E. C. Neeve, D. C. Apperley, R. Bertermann, F. Mo, D. Qiu, M. S. Cheung, L. Dang, J. Wang, U. Radius,Z. Lin, C. Kleeberg, T. B. Marder, *Chem.–Eur. J.*, **2015**, *21*, 7082.
16. A. M. Mfuh, J. D. Doyle, B. Chhetri, H. D. Arman, O. V. Larionov, *J. Am. Chem. Soc.*, **2016**, *138*, 2985.
17. L. Candish, M. Teders, F. Glorius, *J. Am. Chem. Soc.*, **2017**, *139*, 7440.
18. A. Fawcett, J. Pradeilles, Y. Wang, T. Mutsuga, E. L. Myers, V. K. Aggarwal, *Science*, **2017**, *357*, 283.
19. W. F. Florian, S. Armido, *Chem. Sci.*, **2019**, *10*, 8503.
20. K. Chen, S. Zhang, P. He, P. Li, *Chem. Sci.*, **2016**, *7*, 3676.
21. M.J. Frisch, G.W. Trucks, H.B. Schlegel, G.E. Scuseria, M.A. Robb, J.R. Cheeseman, G. Scalmani, V. Barone, B. Mennucci, G.A. Peters-son, H. Nakatsuji, M. Caricato, X. Li, H.P. Hratchian, A.F. Izmaylov, J. Bloino, G. Zheng, J.L. Sonnenberg, M. Hada, M. Ehara, K. Toyota, R. Fukuda, J. Hasegawa, M. Ishida, T. Nakajima, Y. Honda, O. Kitao, H. Nakai, T. Vreven, J.A.,Jr. Montgomery, J. E. Peralta, F. Ogliaro, M. Bearpark, J.J.

Heyd, E. Brothers, K.N. Kudin, V.N. Staroverov, R. Kobayashi, J. Normand, K. Raghavachari, A. Rendell, J.C. Burant, S.S. Iyengar, J. Tomasi, M. Cossi, N. Rega, J.M. Millam, M. Klene, J.E. Knox, J.B. Cross, V. Bakken, C. Adamo, J. Jaramillo, R. Gomperts, R.E. Stratmann, O. Yazyev, A.J. Austin, R. Cammi, C. Pomelli, J.W. Ochterski, R.L. Martin, K. Morokuma, V. G. Zakrzewski, G.A. Voth, P. Salvador, J.J. Dannenberg, S. Dapprich, A.D. Daniels, O. Farkas, J.B. Foresman, J.V. Ortiz, J. Cioslowski, D.J. Fox, Gaussian 09, Revision D.01; Gaussian, Inc.: Wallingford, CT, **2013**.

22. A.D. Becke, *J. Chem. Phys.*, **1993**, *98*, 5648.
23. C. Lee, W. Yang, R.G. Parr, *Phys. Rev. B*, **1988**, *37*, 785.
24. P.J. Stephens, F.J. Devlin, C.F. Chabalowski, M.J. Frisch, *J. Phys. Chem.*, **1994**, *98*, 11623.
25. M. Dolg, U. Wedig, H. Stoll, H. Preuss, *J. Chem. Phys.*, **1987**, *86*, 866.
26. K. Fukui, *Acc. Chem. Res.*, **1981**, *14*, 363.
27. A.V. Marenich, C.J. Cramer, D.G. Truhlar, *J. Phys. Chem. B*, **2009**, *113*, 6378.
28. S. Grimme, J. Antony, S. Ehrlich, H. Krieg, *J. Chem. Phys.*, **2010**, *132*, 154104.
29. R. A. Marcus, *J. Chem. Phys.*, **1956**, *24*, 966.
30. R. A. Marcus, *J. Chem. Phys.*, **1957**, *26*, 872.
31. V. Lemaur, M. Steel, D. Beljonne, J.-L. Brédas, J. Cornil, *J. Am. Chem. Soc.*, **2005**, *127*,6077.
32. J.P. Foster, F. Weinhold, *J. Am. Chem. Soc.*, **1980**, *102*, 7211.
33. (b) A.E. Reed, F. Weinhold, *J. Chem. Phys.* **1983**, *78*, 4066.
34. J. E. Carpenter, F. Weinhold, *J. Mol. Struct. Theochem.*, **1988**, *169*, 41.
35. E.D. Glendening, A.E. Reed, J.E. Carpenter, F. Weinhold, NBO Version 3.1.
36. W. J. Grigsby, P. Power, *Chem.–Eur. J.*, **1997**, *3*, 368.
37. Y. Cheng, C. Mück-Lichtenfeld, A. Studer, *J. Am. Chem.Soc.*, **2018**, *140*, 6221.
38. G. Wang, H. Zhang, J. Zhao, W. Li, J. Cao, C. Zhu, S. Li, *Angew. Chem.*, **2016**, *128*, 6089.
39. L. Zhang, L. Jiao, *Chem. Sci.*, **2018**, *9*, 2711.
40. Y. Zhang, J. Xu, H. Guo, *Org. Lett.*, **2019**, *21*, 9133.
41. Z. Zhang, X. Li, Y. Li, Y. Guo, X. Zhao, Y. Yan, K. Sun, G. Zhang, *Tetrahedron*, **2019**, *75*, 3628.
42. Y. Zhao, W, Xia, *Org. Biomol. Chem.*, **2019**, *17*, 4951.
43. T. Constantin, F. Juliá, N. S. Sheikh, D. Leonori, *Chem. Sci.*, **2020**, *11*, 12822.